

Glueball matrix elements: a lattice calculation and applications

Harvey B. Meyer

*Center for Theoretical Physics
Massachusetts Institute of Technology
Cambridge, MA 02139, U.S.A.
E-mail: meyerh@mit.edu*

ABSTRACT: We compute the matrix elements of the energy-momentum tensor between glueball states and the vacuum in $SU(3)$ lattice gauge theory and extrapolate them to the continuum. These matrix elements may play an important phenomenological role in identifying glue-rich mesons. Based on a relation derived long ago by the ITEP group for J/ψ radiative decays, the scalar matrix element leads to a branching ratio for the glueball that is at least three times larger than the experimentally observed branching ratio for the f_0 mesons above 1GeV. This suggests that the glueball component must be diluted quite strongly among the known scalar mesons. Finally we review the current best continuum determination of the scalar and tensor glueball masses, the deconfining temperature, the string tension and the Lambda parameter, all in units of the Sommer reference scale, using calculations based on the Wilson action.

KEYWORDS: Lattice QCD.

1. Introduction

SU(N) gauge theories in 3+1 dimensions have been studied by lattice Monte-Carlo techniques a long time [1]. Many low-energy dimensionless quantities are now known at the percent level for $N = 3$, as we shall review. However, low-energy matrix elements of local operators have not been given much attention. This is mainly because the lowest possible dimension for a local gauge invariant operator is four. For Monte-Carlo simulations, asymptotic freedom then implies that the amount of statistics has to grow like a^{-4} to maintain fixed relative errors on the matrix elements [2] (a is the lattice spacing). This comes on top of the unavoidable a^{-4} cost of simulating a four-volume fixed in physical units. In particular it is very expensive to take the continuum limit of renormalized matrix elements of the energy-momentum tensor, as is well known to thermodynamics practitioners. In this paper we compute the matrix elements of the energy-momentum tensor between the vacuum on the left and a scalar or tensor glueball on the right. By using a *locally* (i.e. on the scale of one lattice spacing) smoothened gauge field, we are able to reduce the prefactor of the $\sim a^{-4}$ cost function to a manageable size.

While these matrix elements have been computed previously [3], our technology differs. In particular our lattice spacings are significantly smaller and we improve on the statistical accuracy of the matrix elements in the continuum by a factor of about two. This improvement is due mainly to the reduced uncertainty on the non-perturbative normalization factors of the energy-momentum tensor.

One of our motivations is the possibility to confront model predictions with the lattice data. Indeed there are QCD sum rule predictions for these matrix elements [4]. Furthermore, models of QCD based on the AdS/CFT correspondence readily predict many stable glueballs [5], but the spectrum of the SU(3) theory contains only two scalar and two tensor strictly stable glueballs, and this is likely true at any finite number of colors N . By contrast, the detailed properties of the low-lying states, beyond their mass, represent opportunities for unambiguous comparisons. The ability of the energy-momentum tensor to annihilate a glueball is a quantity of this type. Such matrix elements are somewhat analogous to F_π , which determines the width for the $\pi^+ \rightarrow \mu^+ \nu$ decay.

Two other applications will be discussed in section 4. A long time ago the ITEP group derived an approximate expression [4] for the branching ratio for a J/ψ to decay into a scalar glueball in terms of the matrix element that we compute in this paper. We can thus roughly estimate the expected production rate and compare to the experimental branching ratios for scalar mesons.

Secondly we show how the tensor and scalar matrix elements can be used to constrain the thermal spectral functions that determine respectively the shear and bulk viscosity of the plasma of gluons [6, 7].

In section 2 we define the matrix elements to be computed, and give the relation between the lattice observables and the continuum, relativistically covariant quantities. Section 3 describes the lattice calculation. In section 4 we compare our results with those of [3] and present the aforementioned applications. We end with a summary of the current knowledge of the low-energy properties of SU(3) gauge theory.

2. Definitions

In this section we fix our notation, define the relevant matrix elements and show how they can be obtained from Euclidean correlation functions.

2.1 Glueball matrix elements in the continuum

Decomposing the energy-momentum tensor $T_{\mu\nu}$ into a traceless part $\theta_{\mu\nu}$ and a scalar part θ via $T_{\mu\nu} = \theta_{\mu\nu} + \frac{1}{4}\delta_{\mu\nu}\theta$, the explicit Euclidean expressions are

$$\theta(x) \equiv \beta(g)/(2g) F_{\rho\sigma}^a(x) F_{\rho\sigma}^a(x) \quad \theta_{\mu\nu}(x) \equiv \frac{1}{4}\delta_{\mu\nu} F_{\rho\sigma}^a F_{\rho\sigma}^a - F_{\mu\alpha}^a F_{\nu\alpha}^a. \quad (2.1)$$

The beta-function is defined by $qd\bar{g}/dq = \beta(\bar{g}) = -\bar{g}^3(b_0 + b_1\bar{g}^2 + \dots)$ and $b_0 = 11N/(3(4\pi)^2)$, $b_1 = 34N^2/(3(4\pi)^4)$ in the $SU(N)$ pure gauge theory. The gauge action reads $S_g = \frac{1}{4}F_{\mu\nu}^a F_{\mu\nu}^a$ in this notation.

We take over the notation of [3] and define the matrix elements

$$\langle \Omega | \theta(x) | S, p \rangle_r = s e^{-ip \cdot x} \quad (2.2)$$

$$\langle \Omega | \theta_{12}(x) | T, p, \sigma_- \rangle_r = \langle \Omega | \frac{1}{2}(\theta_{11} - \theta_{22})(x) | T, p, \sigma_+ \rangle_r = t e^{-ip \cdot x}, \quad \mathbf{p} = (0, 0, p_3), \quad (2.3)$$

where $|S\rangle$ and $|T\rangle$ respectively refer to the lightest scalar and tensor glueball states. The labels σ_{\pm} refer to the superpositions of helicity states $|\sigma_+\rangle \propto | +2 \rangle + | -2 \rangle$ and $|\sigma_-\rangle \propto | +2 \rangle - | -2 \rangle$. We define s' and t' in the same way for the first excited glueball in each of these channels. The subscript ‘r’ (relativistic) indicates that the state has a Lorentz-invariant normalization,

$${}_r \langle U p \sigma | U q \sigma' \rangle_r = 2p^0 (2\pi)^3 \delta(\mathbf{p} - \mathbf{q}) \delta_{\sigma\sigma'}, \quad U = S, T. \quad (2.4)$$

2.2 Glueball matrix elements from Euclidean correlation functions

We now discuss the extraction of glueball matrix elements from correlation functions in the Euclidean theory, set up in a finite (but large) spatial volume. Separately for the scalar and the tensor channels, we consider the correlation matrix

$$A_{ij}(\tau) = L^{-3} \langle \mathcal{O}_i(0) \mathcal{O}_j(\tau) \rangle_c, \quad i, j = 0, 1, \dots, N_o. \quad (2.5)$$

The subscript ‘c’ indicates that we are dealing with the connected part and τ is the Euclidean time variable. Let us consider first the scalar channel. The operator with label 0 is the definite-momentum projected local current,

$$\mathcal{O}_0(\tau) = \int d^3x e^{i\mathbf{p} \cdot \mathbf{x}} \theta(\tau, \mathbf{x}). \quad (2.6)$$

Operators 1 through N_o are definite-momentum glueball operators, typically extended and designed to have large overlaps on the lightest two states. In finite volume the spectral representation of (2.5) reads

$$A_{ij}(\tau) = \sum_{n=1}^{\infty} \langle \Omega | \mathcal{O}_i | n \rangle \langle n | \mathcal{O}_j | \Omega \rangle e^{-E_n \tau} \quad (2.7)$$

where states are normalized as in quantum mechanics, $\langle n|m \rangle = \delta_{nm}$ and have momentum \mathbf{p} by momentum conservation. In the infinite volume limit, the connection between the first state $|1\rangle$ with the one-particle state $|S, p\rangle_r$ introduced above is

$$\sqrt{2E_{\mathbf{p}}L^3} |1\rangle \rightarrow |S, p\rangle_r, \quad (2.8)$$

where $E_{\mathbf{p}}^2 = M_S^2 + \mathbf{p}^2$. In particular, at large Euclidean time τ ,

$$A_{00}(\tau) = F_S^2 e^{-E_{\mathbf{p}}\tau} + F_{S'}^2 e^{-E'_{\mathbf{p}}\tau} + \mathcal{O}(e^{-E''_{\mathbf{p}}\tau}). \quad (2.9)$$

with

$$F_S(L) \equiv L^{-3/2} |\langle 0|\mathcal{O}_0|1\rangle| \quad \text{and} \quad \lim_{L \rightarrow \infty} F_S(L) = \frac{s}{\sqrt{2E_{\mathbf{p}}}} \quad (2.10)$$

and similarly for the excited state $|2\rangle$ which in the infinite volume limit has energy $E_{\mathbf{p}}'^2 = M_{S'}^2 + \mathbf{p}^2$.

In the tensor channel, similar equations apply as long as \mathbf{p} is collinear with the polarization axis. On the lattice, the equality between the two forms of Eq. 2.3 is violated by $\mathcal{O}(a^2)$ discretization errors as well as finite-size effects. Here we use the second form exclusively, but we perform checks for both sources of systematic error.

In the following we will only use $\mathbf{p} = 0$.

3. Lattice calculation

We simulate the SU(3) gauge theory using the Wilson plaquette action [8] at three values of the bare coupling, $\beta = 6/g_0^2 = 6.0, 6.2$ and 6.408 . This corresponds to values of the Sommer parameter $r_0/a = 5.368(35), 7.383(55)$ and $9.845(85)$ [9]. The lattice size is respectively $16^3 \times 24$, 20^4 and 28^4 . On the coarsest lattice, we also check for finite-volume effects by performing an additional simulation on a $20^3 \times 24$ lattice. The glueball spectrum was determined rather accurately in [10] at these lattice spacings. At the smallest lattice spacing, we apply a conversion factor (given by the ratio of r_0 values) to convert the spectrum from $\beta = 6.4$ to $\beta = 6.408$. We use the standard combination of heatbath and overrelaxation [11, 12, 13, 14] sweeps for the update in a ratio increasing from 3 to 5 as the lattice spacing is decreased. The overall number of sweeps between measurements was also increased, from 8 to 12.

We use the ‘HYP-plaquette’ discretization of the energy-momentum tensor, as described in [15]. We determine its normalization non-perturbatively, following the same strategy as in [15]. The normalization of the discretization based on the bare plaquette is fixed by lattice sum rules, as is well-known in the context of thermodynamics [16]. It is therefore sufficient to determine the normalization of the discretization based on the HYP-plaquette, which we employ here, relative to the bare plaquette. A straightforward way to do this is to match the pressure and energy density computed with either discretization at a specific temperature. The choice $T = 1.21T_c$ made in [15, 2] insures that a large signal is obtained for $\langle \theta \rangle$ and that $T^{-4} \langle \theta_{00} \rangle$ is already more than half its Stefan-Boltzmann limit. Secondly, this choice implies $N_\tau \geq 6$ for $\beta \geq 6.0$, so that large cutoff effects are avoided.

β	$\chi_s(g_0)$	$\chi(g_0)$					
6.000	0.9951(77)	0.5489(68)	β	aM_S	aM_S^*	aM_T	aM_T^*
6.093	0.9778(89)	0.546(14)	6.000	0.7005(47)	1.167(25)	1.0596(64)	1.433(14)
6.180	0.976(12)	0.596(20)	6.100	0.6021(85)	1.038(15)	0.916(11)	1.180(34)
6.295	0.953(20)	0.563(28)	6.200	0.5197(51)	0.929(10)	0.7784(79)	1.032(20)
6.408	0.985(42)	0.612(49)	6.400	0.3960(93)	0.690(18)	0.5758(32)	0.795(28)

Table 1: Left: normalization factors for the HYP-smearred plaquettes relative to the bare plaquette. Right: the glueball masses from [10] relevant to this work.

These relative normalization factors, denoted by $\chi_s(g_0)$ and $\chi(g_0)$ respectively for θ and θ_{00} , are given in table 1. The data is conveniently parametrized as ($6 \leq 6/g_0^2 \leq 6.408$)

$$\chi_s(g_0) = 0.9731 + 0.67(g_0^2 - 6/6.18) \quad (3.1)$$

$$\chi(g_0) = 0.5701 - 0.77(g_0^2 - 6/6.18). \quad (3.2)$$

In both cases, the absolute error increases from 0.007 at $\beta = 6$ to 0.020 at $\beta = 6.408$. We extract $dg_0^{-2}/d\log a$ from the parametrization of $\log(r_0/a)$ given in [9] and use the parametrization of $Z(g_0)$ given in [6].

We employ linear combinations of Wilson loops that project in the A_1^{++} and E^{++} irreducible representations of the cubic group. They are constructed from spatial links variables, using smearing and blocking as described in [17].

3.1 Extraction of the glueball matrix elements

The glueball matrix elements can be extracted at sufficiently large τ using the fit ansatz

$$\hat{A}_{ij}(\tau) = \sum_{n=1,2} c_n^{(i)} c_n^{(j)} e^{-M_n \tau} \quad (3.3)$$

$$\Rightarrow F_U = |c_1^{(0)}|, \quad F_{U'} = |c_2^{(0)}|, \quad U = S, T. \quad (3.4)$$

A few remarks are in order:

- the correlator A_{00} is not included in the fit.
- in our discretization the operator \mathcal{O}_0 is defined at half-integer times (in lattice units); thus for $i \geq 1, j = 0$, τ/a takes half integer values in (3.3), whereas for $i, j \geq 1$ it takes integer values.
- the glueball spectrum is already accurately known at the same simulations parameters from ([10], Table 7.1). We reproduce the values \overline{M}_n in table 1 and treat them as a ‘prior’.

Note however that since this information is exact within its quoted error, it is unnecessary to invoke Bayesian arguments to make use of it. Therefore we determine the fit parameters

by minimizing $\chi^2 = \chi_I^2 + \chi_{II}^2$, with

$$\chi_I^2 = \sum_{\substack{i \leq j \\ k \leq l}} \sum_{\tau=u_{ij}}^{v_{ij}} \sum_{\tau'=u_{kl}}^{v_{kl}} [A_{ij}(\tau) - \hat{A}_{ij}(\tau)] C^{-1}_{(ij\tau),(kl\tau')} [A_{kl}(\tau') - \hat{A}_{kl}(\tau')] \quad (3.5)$$

$$\chi_{II}^2 = \sum_{n=1,2} \frac{(M_n - \overline{M}_n)^2}{\sigma_n^2}. \quad (3.6)$$

We use the full correlation matrix C in this fit. Autocorrelation effects in Monte-Carlo time were found to be negligible, so that $C_{(ij\tau),(kl\tau')}$ could be taken to be the usual estimator of $N_{\text{mst}}^{-1}[\langle A_{ij}(\tau)A_{kl}(\tau') \rangle - \langle A_{ij}(\tau) \rangle \langle A_{kl}(\tau') \rangle]$, where $\langle \cdot \rangle$ are path integral averages and N_{mst} is the number of measurements. We estimated the relative error on the eigenvalues of C and found them to be small, due to the high statistics of the calculation. This makes the inversion of C a stable procedure.

We used two non-local operators in the fits, i.e. the indices $i, j, k, l \leq 2$ in Eq. 3.5. These operators were linear combinations of non-local operators in the relevant lattice irreducible representation designed to have a good projection on the lightest two states. Increasing the number of operators in the fit did not seem to improve the determination of the physical parameters. The results and minimized χ^2 of these fits are given in Table 2. The χ^2 are of order unity, with a tendency to be slightly larger than one. This may be due (partly) to the fact that the standard estimator for the χ^2 we are using is an upward-biased one [18]. Beyond the value of the χ^2 it is important to check that the fit is stable against variations in the fit ranges $u_{ij} \leq \tau \leq v_{ij}$, and that no strong trend is seen in $A_{ij}(\tau)/\hat{A}_{ij}(\tau)$ as a function of τ within the fit range. Figure 1 displays this ratio in the scalar and in the tensor sectors for the simulation at the smallest lattice spacing. We see that the correlators A_{01} and A_{11} have small deviations from the fit even outside the fit range. This gives us confidence that excited state ($n \geq 3$) contaminations are negligible in the fit range. This property is much less satisfied for the A_{02} and A_{22} correlators. Although the fit range for the correlators starts further out in τ , this implies that the control over excited state contributions is much less good for F_{S^*} and F_{T^*} . We will therefore not include these matrix elements in our final list of results.

We may use the effective mass and the effective matrix element

$$am_{\text{eff}}(t) = \log \frac{A_{11}(\tau)}{A_{11}(\tau + a)}, \quad (3.7)$$

$$F_{U,\text{eff}}(\tau - \frac{1}{2}a) = A_{01}(\tau - \frac{1}{2}a) \frac{A_{11}(\tau - a)^{(\tau-a)/2a}}{A_{11}(\tau)^{\tau/2a}}, \quad U = S, T, \quad \tau = 2a, 3a, \dots \quad (3.8)$$

as a way to visualize the contributions of excited states to the physical quantities we extract (see Fig. 2). The effective quantities computed from the fit to the correlators (Eq. 3.5, 3.6) are also shown as curves on the plot. The fit looks convincing. We find that, in general, the method of determining the mass and matrix elements from the effective quantities is less stable than fitting the correlators. A possible reason for this is that the histograms of ratios as in Eq. 3.8 can become arbitrarily non-Gaussian if the denominator is noisy (e.g. at large τ), even if the correlators were perfectly Gaussian distributed.

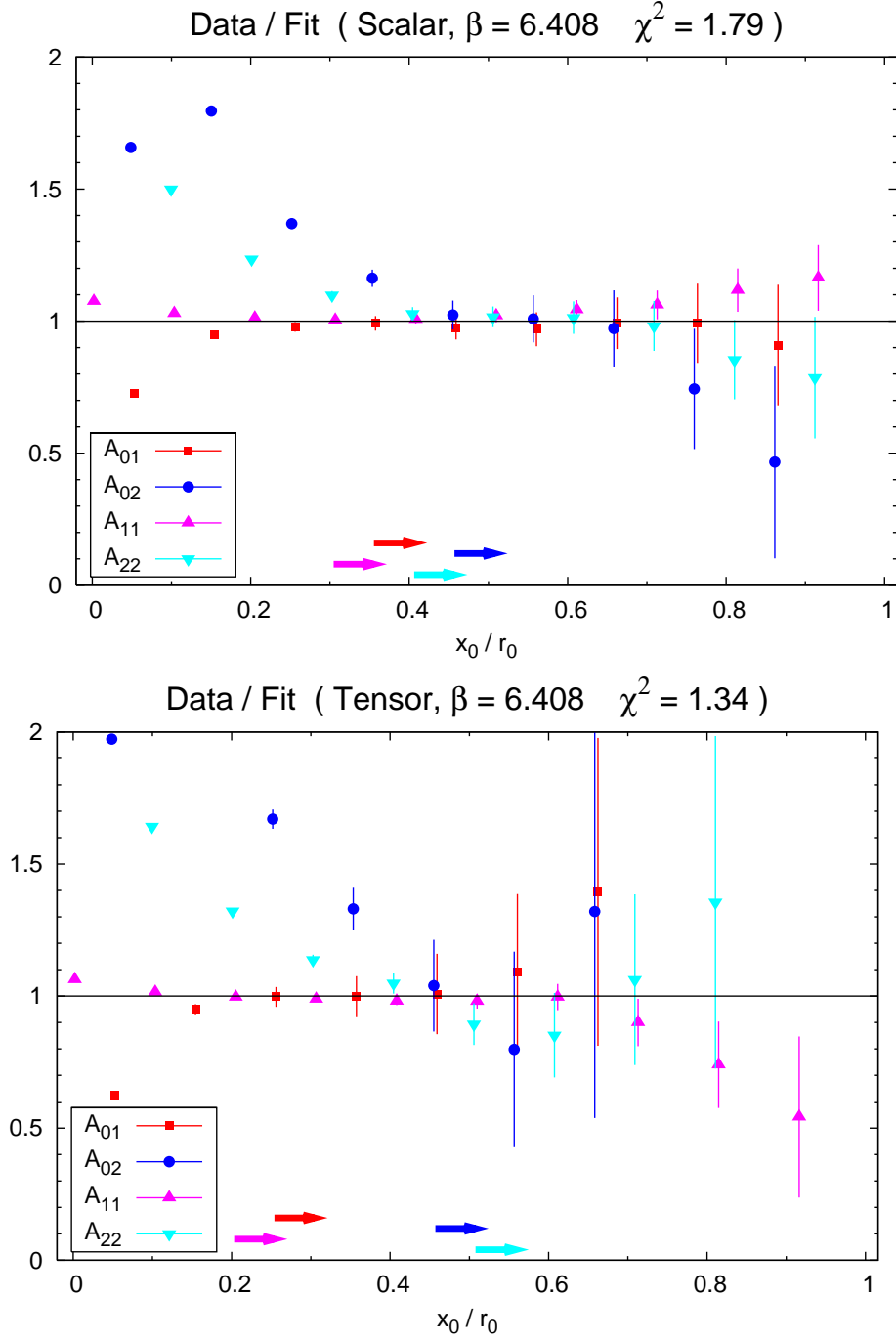


Figure 1: The ratio of the scalar (top) and tensor (bottom) correlators to the fit, Eq. 3.3. The arrows indicate for each correlator where the fit starts.

Finally, increasing the volume from 16^3 to 20^3 at $\beta = 6.0$ does not affect the matrix elements in a statistically significant way (see Tab.2). An effect at the subpercent level is seen on some of the glueball masses, because they are so accurately determined, but this does not affect the discussion in the rest of this paper.

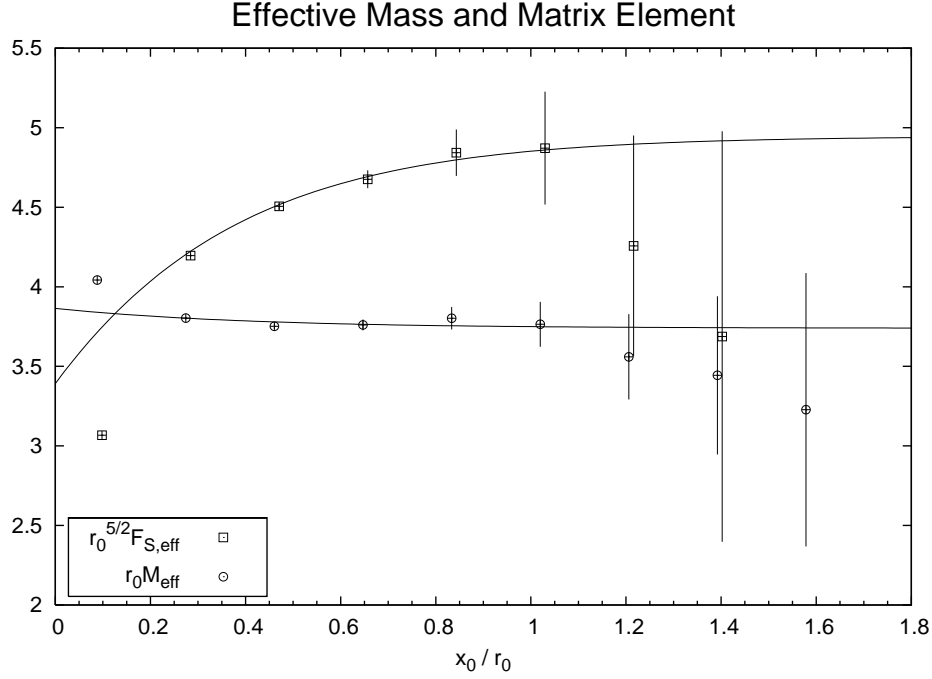


Figure 2: The effective mass and matrix element in the scalar sector at $\beta = 6$, $16^3 \times 24$ lattice. The fit Eq. 3.3 is shown. The fit starts at $x_0 = a \approx 0.19r_0$ for the diagonal correlator and at $x_0 = \frac{5}{2}a \approx 0.47r_0$ for the correlator between the local and the smeared operator.

β	aM_S	aM_{S^*}	aM_T	aM_{T^*}
6.000 (20^3)	0.7032(16)	1.1733(37)	1.0587(15)	1.43261(53)
6.000 (16^3)	0.6966(16)	1.1747(58)	1.0592(22)	1.4358(10)
6.200	0.51918(96)	0.93010(30)	0.7783(20)	1.0399(22)
6.408	0.39603(63)	0.6946(11)	0.5937(36)	0.8322(92)

β	$F_S r_0^{5/2}$	$F_{S^*} r_0^{5/2}$	χ^2/ν	$F_T r_0^{5/2}$	$F_{T^*} r_0^{5/2}$	χ^2/ν
6.000 (20^3)	5.05(06)(09)	6.53(30)(12)	1.33	3.63(26)(08)	8.49(78)(27)	1.29
6.000 (16^3)	4.95(03)(09)	6.21(19)(12)	1.36	3.41(11)(08)	7.72(40)(25)	0.94
6.200	4.43(25)(09)	10.25(90)(22)	1.50	3.07(32)(09)	10.37(68)(29)	1.29
6.408	4.55(36)(14)	9.75(54)(31)	1.79	2.30(33)(10)	11.04(38)(48)	1.34

Table 2: The scalar (S) and tensor (T) glueball masses and matrix elements extracted from the fits. In the lower table, the first error is the uncertainty coming from the bare matrix element in lattice units, the second is the cumulated error of all the other factors entering the renormalization group invariant quantity.

3.2 Continuum extrapolation

Having obtained the matrix elements at three different lattice spacings, we can attempt a

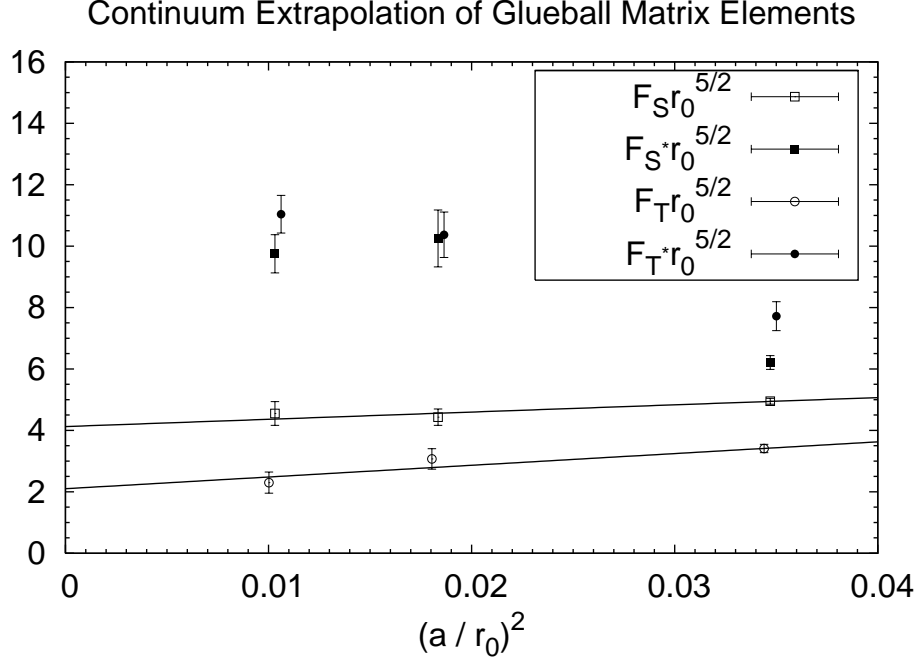


Figure 3: Continuum extrapolation.

continuum extrapolation linear in $(a/r_0)^2$, as illustrated on Fig. 3. We find

$$F_{S'r_0}^{5/2} = 4.13(40), \quad \chi^2/\text{d.o.f.} = 0.46 \quad (3.9)$$

$$F_{T'r_0}^{5/2} = 2.10(41), \quad \chi^2/\text{d.o.f.} = 0.99 \quad (3.10)$$

The extrapolations are satisfactory: the χ^2 is small, the slopes of the extrapolations are small to moderate. In particular the continuum value is statistically compatible with the value from the smallest lattice spacing.

We do not attempt an extrapolation for the first excited states. Indeed it is clear from Fig. 3 that the $\beta = 6.0$ data does not lie in the a^2 scaling region. The values from the lighter two lattice spacings are consistent with each other, suggesting that cutoff effects are small beyond $\beta = 6.2$. Our best estimate of $F_{S'r_0}^{5/2}$ and $F_{T'r_0}^{5/2}$ are thus the values at the smallest lattice spacing, but one should keep in mind that our control over excited state contamination is far less good for these matrix elements; the induced systematic uncertainty is comparable or larger than the statistical error.

4. Applications and summary

In the following, we compare our results to previously obtained ones. Then we present two applications of the computed matrix elements. We end with a summary of our knowledge of non-perturbative dimensionless ratios in the SU(3) gauge theory.

4.1 Technical comparison

We can compare our results to those of [3]. We find¹,

$$\text{this work} \quad \text{Chen et al.} \quad (4.1)$$

$$sr_0^3 = 11.6(1.1) \quad 15.8(3.2) \quad (4.2)$$

$$tr_0^3 = 7.1(1.4) \quad 7.5(2.8) \quad (4.3)$$

Comparing the matrix elements in units of r_0 saves us from having to settle on a value for r_0 in fm ($r_0^{-1} = 410\text{MeV}$ was used in [3]). We conclude that our results are in satisfactory agreement with those of [3], and the statistical uncertainties have been reduced by a factor of at least two.

We stress that while our continuum extrapolation uses data at lattice spacings $(a/r_0)^2$ in the range 0.010 to 0.035, the continuum extrapolation of [3] uses data in the range of spatial lattice spacings 0.044 to 0.22. The control of the continuum limit is thus qualitatively different. One might worry that the support of the field strength operators used for the ‘type II’ discretization in [3] varies between 0.4fm and 0.9fm. On the other hand, the authors do find good agreement between certain observables which only become strictly equal in the continuum limit.

We have used non-perturbative renormalization factors at every lattice spacing, while the procedure used in [3] for s and t implies that the continuum is approached asymptotically with $O(g_0^2)$ as well as $O(a^2)$ corrections.

Simulating at small lattice spacings comes at a heavy computational price for these observables: the signal-to-noise ratio for matrix elements of the gluonic dimension four operators decreases with the fourth power of the lattice spacing [2]. This explains why our statistical errors on the bare matrix elements are somewhat larger than in [3].

The use of a coarse spatial lattice allowed the authors of [3] to reach volumes significantly larger than ours in physical units. We have however checked for finite volume effects explicitly, and find no significant variation in the matrix elements. It is known [19] that the low-lying spectrum of glueballs exhibits remarkably small finite-size effects for $L > 2.5r_0$ (and for certain channels they remain small for even smaller box sizes).

4.2 Glueball production rate in radiative J/ψ decays

First of all, we can compare our result for s with the QCD sum rule prediction [4]

$$s \approx \frac{11}{4\pi} \sqrt{\frac{G_0}{2b_0}} M_S. \quad (4.4)$$

Using $G_0 = 0.012\text{GeV}^4$ (the ‘gluon condensate’) and $r_0^{-1} = 410\text{MeV}$ this leads to $sr_0^3 \approx 6.0$, almost a factor two smaller than our result. Since we regard the gluon condensate as a phenomenological parameter, this disagreement does not surprise us too much.

We may use our value for s to estimate the partial width of J/ψ to radiatively decay into a scalar glueball. An approximate expression for this experimentally observable quantity

¹As compared to [3], our s contains an extra factor of $11/(4\pi)^2$ (coming from the beta-function).

was derived in [4],

$$\Gamma(J/\psi \rightarrow G_0\gamma) \approx \frac{8\pi\alpha^3}{5^2 \cdot 11^2 \cdot 3^8} \frac{m_{J/\psi}^4 s^2}{m_c^8 \Gamma(J/\psi \rightarrow e^+e^-)}. \quad (4.5)$$

Here $m_c \simeq 1250\text{MeV}$ is the charm mass in the $\overline{\text{MS}}$ scheme at scale $\mu = m_c$, $m_{J/\psi} \simeq 3097\text{MeV}$ is the J/ψ mass, $\alpha \simeq \frac{1}{137}$ is the fine structure constant and $\Gamma(J/\psi \rightarrow e^+e^-) \simeq 5.55\text{keV}$. The ingredients that go into this formula are the $1/m_c$ expansion, a dispersion relation for the charm-quark loop induced $\gamma\gamma \rightarrow gg$ transition and the assumption that the J/ψ contribution dominates the spectral integral. This leads to the estimate

$$\text{Br}(J/\psi \rightarrow G_0\gamma) \approx 0.009. \quad (4.6)$$

The authors of [4] also suggest that a more accurate prediction is

$$\text{Br}(J/\psi \rightarrow G_0\gamma) = \left(\frac{3\pi}{11}\right)^2 \frac{s^2 \cdot \text{Br}(J/\psi \rightarrow \eta'\gamma)}{|\langle\Omega|\alpha_s F_{\mu\nu}^a \tilde{F}_{\mu\nu}^a|\eta'\rangle|^2}. \quad (4.7)$$

Here the assumption about the dominance of the J/ψ is replaced by the assumption that the relative size of the J/ψ and the ‘continuum’ contributions are identical in the scalar and the pseudoscalar channels. Using Eq. (5) of [20], we can trade the properties of η' for the corresponding ones for η and use the $SU(3)_f$ result [20]

$$\langle\Omega|\alpha_s F_{\mu\nu}^a \tilde{F}_{\mu\nu}^a|\eta\rangle = \frac{4\pi}{3} \sqrt{\frac{3}{2}} f_\eta m_\eta^2 \quad (4.8)$$

with $f_\eta \approx 170\text{MeV}$. Then we obtain

$$\text{Br}(J/\psi \rightarrow G_0\gamma) \approx \frac{3^3}{11^2 \cdot 2^3} \left(\frac{1-x'^2}{1-x^2}\right)^3 \frac{s^2 \cdot \text{Br}(J/\psi \rightarrow \eta\gamma)}{f_\eta^2 m_\eta^4} = 5.6(1.7) \cdot \text{Br}(J/\psi \rightarrow \eta\gamma). \quad (4.9)$$

Here $x = m_\eta/m_{J/\psi}$ and $x' = m_{\eta'}/m_{J/\psi}$. Since $\text{Br}(J/\psi \rightarrow \eta\gamma) = 0.98(10) \cdot 10^{-3}$ [21], we obtain a somewhat lower result than (4.6). This is still a rather large branching ratio. For instance, the PDG [21] gives $\text{Br}(J/\psi \rightarrow \gamma f_0(1710)) \approx 1.5(3) \cdot 10^{-3}$ if one adds up the contributions of the $\gamma K\bar{K}$, $\gamma\pi\pi$ and $\gamma\omega\omega$ channels. The production rate of $f_0(1500)$ is even smaller. According to (4.9), if any of the $f_0(1370)$, $f_0(1500)$ or $f_0(1710)$ states had a glueball component close to unity, they would be produced more copiously than observed. Therefore, Eq. 4.9 suggests that the glueball component is quite strongly diluted among the three states. This conclusion is also reached by doing detailed parametrizations and fits to experimental data of the mixing pattern [22, 23].

4.3 Constraining thermal spectral functions

Another application arises in the calculation of transport coefficients in the plasma of gluons. Indeed the local-current two-point function A_{00} can be expressed in terms of the spectral function $\rho(\omega, \mathbf{p}, T)$,

$$A_{00}(\tau, \mathbf{p}, T) = \int_0^\infty d\omega \rho(\omega, \mathbf{p}, T) \frac{\cosh \omega(\frac{1}{2T} - \tau)}{\sinh \frac{\omega}{2T}}. \quad (4.10)$$

Here T is the temperature. In the tensor channel the shear viscosity is then given by

$$\eta(T) = \pi \lim_{\omega \rightarrow 0} \frac{\rho(\omega, \mathbf{0}, T)}{\omega}. \quad (4.11)$$

Because A_{00} is dominated by ultraviolet contributions that are temperature independent, in [24] we proposed to subtract from A_{00} what that correlator would be if the spectral function was the same as at $T = 0$, before solving Eq. 4.10 for $\rho(\omega, \mathbf{p}, T)$. Let us call that would-be correlator \tilde{A}_{00} . The $T = 0$ spectral function has a simple expression in terms of energy levels and matrix elements of the kind we calculated in this paper,

$$\rho(\omega, \mathbf{p}, T = 0) = L^{-3} \sum_n \delta(\omega - E_n) |\langle 0 | \mathcal{O}_0 | n \rangle|^2. \quad (4.12)$$

Therefore, we find that the contributions of the first two terms in Eq. 4.12 to $\tilde{A}_{00}(\tau, \mathbf{0}, T)$ read (at $N_t = 1/(aT) = 8$)

$$\tilde{A}_{00}(\tau, \mathbf{0}, 1.24T_c) = 1.25 + 5.2 + \dots \quad (4.13)$$

$$\tilde{A}_{00}(\tau, \mathbf{0}, 1.65T_c) = 0.388 + 3.7 + \dots \quad (4.14)$$

These contributions are substantial since $A_{00}(\tau, \mathbf{0}, T) = 8.05(32)$ and $8.73(33)$ respectively [24]. The first excited state contribution appears to be particularly large. Due to possible higher state contamination in our estimate of F_{S^*} and F_{T^*} (see section 3), it may be that the second terms in Eq. 4.13 or 4.14 effectively amounts to the contribution of more than one state.

4.4 A summary of the low-energy parameters of SU(3) gauge theory

We finish with a summary of our knowledge of low-energy dimensionless quantities in the SU(3) gauge theory. The results we use were all obtained with the Wilson plaquette action [8] and we extrapolate them to the continuum. We use the parametrization of $(r_0/a)(\beta)$ from [9]. If σ is the string tension, T_c the deconfining temperature and $\Lambda_{\overline{\text{MS}}}$ the Lambda parameter in the $\overline{\text{MS}}$ scheme, we find in the continuum

$$M_S r_0 = 3.958(47) \quad \chi^2/(4 - 2) = 0.09, \quad (4.15)$$

$$M_T r_0 = 5.878(77) \quad \chi^2/(4 - 2) = 0.6, \quad (4.16)$$

$$s r_0^3 = 11.6(1.1) \quad \chi^2/(3 - 2) = 0.5, \quad (4.17)$$

$$t r_0^3 = 7.1(1.4) \quad \chi^2/(3 - 2) = 1.0, \quad (4.18)$$

$$\sqrt{\sigma} r_0 = 1.1611(95) \quad \chi^2/(5 - 2) = 0.1, \quad (4.19)$$

$$T_c r_0 = 0.7463(64) \quad \chi^2/(4 - 2) = 0.3, \quad (4.20)$$

$$\Lambda_{\overline{\text{MS}}} r_0 = 0.60(5). \quad (4.21)$$

The data for aM_S , aM_T , sa^3 and ta^3 is from this work, plus the $\beta = 6.1$ glueball mass data from [10]. The string tension $a\sqrt{\sigma}$ is taken from [17] ($\beta \geq 5.8000$) and from [10] ($\beta = 6.4$). We took the critical values of β for given $N_t = 1/(aT)$ from [25] ($N_t = 6, 8, 12$) and from [26] ($N_t = 5$). The Lambda parameter value is the data of [27]. We do a continuum extrapolation linear in $(a/r_0)^2$ for the first five quantities. We extrapolate $T_c r_0$ as a function of $1/N_t^2$. The quantity $\Lambda_{\overline{\text{MS}}} r_0$ is already given in the continuum in [27].

The overall level of accuracy achieved is remarkable.

5. Conclusion

In summary, we have computed scalar and tensor glueball matrix elements in $SU(3)$ gauge theory with improved precision. A straightforward application to the production of scalar glueballs in J/ψ radiative decays suggests that none of the known scalar mesons can contain too large a glueball component. Finally we gave a summary of the current knowledge of seven non-perturbative observables of the $SU(3)$ gauge theory. We hope that these quantities constitute a useful set for models and semi-analytical methods to calibrate on and compare predictions to.

Acknowledgments

The simulations were done on the desktop machines of the Laboratory for Nuclear Science at M.I.T. This work was supported in part by funds provided by the U.S. Department of Energy under cooperative research agreement DE-FG02-94ER40818.

References

- [1] M. Creutz, *Confinement and the Critical Dimensionality of Space- Time*, *Phys. Rev. Lett.* **43** (1979) 553–556.
- [2] H. B. Meyer and J. W. Negele, *The Glue Content of the Pion*, *PoS LATTICE2007* (2007) 154, [[arXiv:0710.0019](#)].
- [3] Y. Chen *et. al.*, *Glueball spectrum and matrix elements on anisotropic lattices*, *Phys. Rev.* **D73** (2006) 014516, [[hep-lat/0510074](#)].
- [4] V. A. Novikov, M. A. Shifman, A. I. Vainshtein, and V. I. Zakharov, *In a Search for Scalar Gluonium*, *Nucl. Phys.* **B165** (1980) 67.
- [5] R. C. Brower, S. D. Mathur, and C.-I. Tan, *Glueball spectrum for QCD from AdS supergravity duality*, *Nucl. Phys.* **B587** (2000) 249–276, [[hep-th/0003115](#)].
- [6] H. B. Meyer, *A calculation of the shear viscosity in $SU(3)$ gluodynamics*, *Phys. Rev.* **D76** (2007) 101701, [[arXiv:0704.1801](#)].
- [7] H. B. Meyer, *A calculation of the bulk viscosity in $SU(3)$ gluodynamics*, *Phys. Rev. Lett.* **100** (2008) 162001, [[arXiv:0710.3717](#)].
- [8] K. G. Wilson, *Confinement of quarks*, *Phys. Rev.* **D10** (1974) 2445–2459.
- [9] S. Necco and R. Sommer, *The $N(f) = 0$ heavy quark potential from short to intermediate distances*, *Nucl. Phys.* **B622** (2002) 328–346, [[hep-lat/0108008](#)].
- [10] H. B. Meyer, *Glueball Regge trajectories*, [hep-lat/0508002](#).
- [11] M. Creutz, *Monte Carlo Study of Quantized $SU(2)$ Gauge Theory*, *Phys. Rev.* **D21** (1980) 2308–2315.
- [12] N. Cabibbo and E. Marinari, *A New Method for Updating $SU(N)$ Matrices in Computer Simulations of Gauge Theories*, *Phys. Lett.* **B119** (1982) 387–390.
- [13] A. D. Kennedy and B. J. Pendleton, *Improved Heat Bath Method for Monte Carlo Calculations in Lattice Gauge Theories*, *Phys. Lett.* **B156** (1985) 393–399.

- [14] K. Fabricius and O. Haan, *Heat Bath Method for the Twisted Eguchi-Kawai Model*, *Phys. Lett.* **B143** (1984) 459.
- [15] H. B. Meyer and J. W. Negele, *Gluon contributions to the pion mass and light cone momentum fraction*, *Phys. Rev.* **D77** (2008) 037501, [[arXiv:0707.3225](#)].
- [16] J. Engels, F. Karsch, H. Satz, and I. Montvay, *High Temperature $SU(2)$ Gluon Matter on the Lattice*, *Phys. Lett.* **B101** (1981) 89.
- [17] B. Lucini, M. Teper, and U. Wenger, *Glueballs and k -strings in $SU(N)$ gauge theories: Calculations with improved operators*, *JHEP* **06** (2004) 012, [[hep-lat/0404008](#)].
- [18] U. Wolff, *private notes*, .
- [19] H. B. Meyer, *The spectrum of $SU(N)$ gauge theories in finite volume*, *JHEP* **03** (2005) 064, [[hep-lat/0412021](#)].
- [20] V. A. Novikov, M. A. Shifman, A. I. Vainshtein, and V. I. Zakharov, *A Theory of the $J/\psi \rightarrow \eta$ (η') γ Decays*, *Nucl. Phys.* **B165** (1980) 55.
- [21] **Particle Data Group** Collaboration, C. Amsler *et. al.*, *Review of particle physics*, *Phys. Lett.* **B667** (2008) 1.
- [22] F. E. Close, G. R. Farrar, and Z.-p. Li, *Determining the gluonic content of isoscalar mesons*, *Phys. Rev.* **D55** (1997) 5749–5766, [[hep-ph/9610280](#)].
- [23] F. E. Close and Q. Zhao, *Production of $f_0(1710)$, $f_0(1500)$, and $f_0(1370)$ in J/ψ hadronic decays*, *Phys. Rev.* **D71** (2005) 094022, [[hep-ph/0504043](#)].
- [24] H. B. Meyer, *Computing the viscosity of the QGP on the lattice*, [arXiv:0805.4567](#).
- [25] G. Boyd *et. al.*, *Thermodynamics of $SU(3)$ Lattice Gauge Theory*, *Nucl. Phys.* **B469** (1996) 419–444, [[hep-lat/9602007](#)].
- [26] B. Lucini, M. Teper, and U. Wenger, *The high temperature phase transition in $SU(N)$ gauge theories*, *JHEP* **01** (2004) 061, [[hep-lat/0307017](#)].
- [27] **ALPHA** Collaboration, S. Capitani, M. Luscher, R. Sommer, and H. Wittig, *Non-perturbative quark mass renormalization in quenched lattice QCD*, *Nucl. Phys.* **B544** (1999) 669–698, [[hep-lat/9810063](#)].